ARTICLE IN PRESS

Available online at www.sciencedirect.com

ScienceDirect

Ceramics International ▮ (▮▮▮▮) ▮▮▮–▮▮▮

CERAMICS INTERNATIONAL

www.elsevier.com/locate/ceramint

# Human mesenchymal stem cell viability, proliferation and differentiation potential in response to ceramic chemistry and surface roughness

Patricia Mazón[a], David García-Bernal[b], Luis Meseguer-Olmo[c,1], Francesca Cragnolini[b], Piedad N. De Aza[d,*]

[a]Departamento de Materiales, Óptica y Tecnologia Electrónica, Universidad Miguel Hernández, Avda. Universidad s/n, 03202 Elche, Alicante, Spain
[b]Instituto Murciano de Investigación Biosanitaria (IMIB), University of Murcia, 30120 Murcia, Spain
[c]Servicio de Cirugía Ortopédica, Unidad de Bioingeniería Ósea, Hospital Clínico Universitario Virgen de la Arrixaca, 30120 Murcia, Spain
[d]Instituto de Bioingeniería, Universidad Miguel Hernández, Avda. Universidad s/n, 03202 Elche, Alicante, Spain

Received 19 September 2014; received in revised form 21 January 2015; accepted 21 January 2015

**Abstract**

We investigated the effect of the ceramic chemistry and surface roughness of pure α-tricalcium phosphate, and also αTCP doped with either 1.5 wt% or 3.0 wt% of dicalcium silicate ($C_2S$), on the response of adult human mesenchymal stem cells (*ah*MSCs). A*h*MSCs were plated onto ceramic discs, prepared by a solid-state reaction. After being sintered, some samples were polished up to 1 μm, while others were kept as manufactured, which resulted in two surface roughness grades. Viability, proliferation and osteoinductive capacity were determined following various incubation periods.

The results showed a non-cytotoxic effect after an indirect apoptosis test. Cell adhesion and proliferation were surface roughness-sensitive and increased proportionally to the roughness of materials. These observations became more evident in the unpolished αTCP ceramic doped with 1.5 wt% $C_2S$, which induced osteoblastic differentiation as a result of the roughness and increased concentration of the $C_2S$ solid solution in αTCP.



*Keywords:* A. Powder solid-state reaction; B. Surfaces; D. Apatite; E. Biomedical applications; Bone regeneration

## 1. Introduction

Surface reactivity is one of the common characteristics of bone bioactive ceramics. It contributes to their bone bonding ability and their enhancing effect on bone tissue formation. During implantation, reactions occur on the material tissue interface, which leads to time-dependent changes in the surface characteristics of the implant material, and also in tissues.

Modification of the biomaterial surface properties by controlling the characteristic length scale (e.g., grain size, crystal phase, etc.) or roughness is a promising approach to modulate selected cell functions.

Tricalcium phosphate, hydroxiapatite, bioglass and wollastonite are usually considered bone bioactive ceramics. These materials are generally bond to surrounding osseous tissue and enhance bone tissue formation [1–5]. Since direct bone bonding to Bioglass was first observed [6], considerable progress has been made in understanding the basic mechanisms of bone-biomaterial bond formation and its effect on bone formation. This progress has resulted mainly from two approaches: one focuses on studying the bone-biomaterials interface that was developed in vivo. An examination of the bonding zone revealed the consistent presence of an interfacial carbohydroxyapatite layer (CHA) [7,8]; in the second approach, *in vitro* immersions were

*Corresponding author. Tel.: +34 966 658 485; fax: +34 96 522 2033.
*E-mail addresses:* pmazon@umh.es (P. Mazón), redond@gmail.com (D. García-Bernal), lmeseguer.doc@gmail.com (L. Meseguer-Olmo), dott.ssa_franci@hotmail.it (F. Cragnolini), piedad@umh.es (P.N. De Aza).
[1]Dept. of Orthopaedic Surgery, Catholic University of Murcia, 30107 Murcia, Spain.

http://dx.doi.org/10.1016/j.ceramint.2015.01.110
0272-8842/

used in simulated physiological fluids or media containing cells [9,10]. These analyses have revealed that some reactions, such as dissolution, precipitation and ion exchange, occur on implant material surfaces. The combination of *in vivo* and *in vitro* studies has led to a better understanding of the surface reactions of bioactive ceramics in the body and their effects on bone formation and cell function.

In general, bone substitute materials of different (natural or synthetic origins) can induce bone formation when combined with multipotent undifferentiated mesenchymal stem cells (hybrid materials). Based on this premise, several tissue engineering approaches have been used to increase the utility of biomaterials for clinical bone repair by including these osteoblastic precursor cells into a scaffold, followed by a period of osteogenic pre-differentiation of these cells in biomaterials before host implantation [11]. Presently, several techniques for the isolation and culture of *ah*MSCs obtained from bone marrow aspirates of human donors are available. Therefore, they represent an ideal source for their use in bone tissue bioengineering. To implement this approach, the selected biomaterial must be capable of allowing adhesion and growth of osteoprogenitor cells, and of promoting osteoblastic differentiation to thereby facilitate the neo-bone formation process.

Cells are able to discriminate subtle differences in surface roughness [12]. Osteoblast-like cells can discriminate between not only surfaces of different roughness, but also surfaces with comparable roughness, but with different topographies [13]. Thus surface morphology is of much importance.

The objectives of the present work were: (1) to evaluate the influence of substrate chemistry and (2) surface roughness on *ah*MSCs behaviour, and (3) to investigate how subtle differences in surface roughness can influence the *in vitro* short- and long-term responses of *ah*MSCs. For this purpose, we analysed the cell adhesion, proliferation, differentiation potential and viability of *ah*MSCs on bioceramic substrates of three chemistries (pure αTCP, and αTCP doped with either 1.5 wt% or 3.0 wt% of $C_2S$ with a well-controlled grain size and crystal phase) with two different surface roughness values.

## 2. Material and methods

### 2.1. Material

The chemicals used in the synthesis of tricalcium phosphate and dicalcium silicate were calcium hydrogen phosphate anhydrous ($CaHPO_4 > 98.0$ wt%, Panreac, Barcelona, Spain), calcium carbonate ($CaCO_3 > 99.0$ wt% Fluka Analytical, St. Gallen, Switzerland) and high-purity silicon oxide ($SiO_2 > 99.7$ wt%, Strem Chemicals, Cambridge, England). Stoichiometric quantities of the raw powders to obtain tricalcium phosphate and dicalcium silicate were ground in a laboratory mixing miller (MM301-Retsch) using PSZ-zirconia balls.

### 2.2. Processing methods

TCP and $C_2S$ were obtained by solid-state reaction sintering. Details of the technique can be found in previous publications [4,14].

The powders obtained were ground and characterised by X-ray fluorescence (XRF), X-ray diffraction (XRD-Bruker AXS D8-Advance X-ray Diffractometer; Karksruhe, Germany) and particle size distribution (Laser diffraction, Mastersizer S Malvern).

The αTCP ceramic and αTCP compositions doped with either 1.5 wt% or 3.0 wt% of $C_2S$ (TCPss) were prepared for this study. The desired proportions of each component were weighed on an analytical balance, dispersed in acetone and thoroughly mixed in a manual agate mortar. The mixture was isostatically pressed into bars at 200 MPa, heated to 1500 °C for 2 h, and followed by liquid nitrogen quenching after rapid removal from the furnace. In order to homogenise compositions, bars were ground, pressed and reheated. This procedure was repeated 3 times. The powders obtained with an average particle size of 23 μm were pressed into bars at 200 MPa. The next step involved heating the bars up to 1500 °C for 4 h, followed by cooling to 1120 °C inside the furnace, where they remained for 16 h before being cooled down to room temperature. Heat treatment temperatures were carefully selected after bearing in mind the information provided by the $\alpha TCP_{ss}$-silicocarnotite subsystem within the binary system of TCP–$C_2S$ [$Ca_3(PO_4)_2$–$Ca_2SiO_4$] [15]. The final samples were cut from the obtained bars, which measured 7 mm in diameter and 1.5 mm in thickness.

Two different surface roughness types were produced: the first performed by a cutting machine, with which an opaque surface was obtained; the second produced by sequential polishing with 6 μm and 1 μm diamond pastes, with which a bright mirror-like surface was obtained.

### 2.3. Material and surface characterisation

#### 2.3.1. Powder X-ray diffraction

XRD were obtained using an automated diffractometer. They were compared with the database provided by the Joint Committee on Powder Diffraction Standards (JCPDS).

#### 2.3.2. Surface profilometry

The surface roughness of the pure αTCP, and also the αTCP doped with either 1.5 wt% or 3.0 wt% of $C_2S$ disks, was measured by profilometry in a Mitutoyo SJ-201P profilometer. Five disks of each material with the different roughness values were measured to obtain an average roughness value $R_a$. Five individual measurements were taken on each specimen. The statistically significant differences in the Ra values were determined by an ANOVA statistical analysis. Differences were considered significant when $p < 0.05$.

#### 2.3.3. Scanning electron microscopy

Scanning electron microscopy (SEM-Hitachi S-3500N), equipped with an Energy Dispersive X-ray Spectrometer (EDX) microanalysis probe (INCA-Oxford), was used to investigate the morphology and texture of surfaces, and the semiquantitative analysis of surface composition.

Please cite this article as: P. Mazón, et al., Human mesenchymal stem cell viability, proliferation and differentiation potential in response to ceramic chemistry and surface roughness, Ceramics International (2015), http://dx.doi.org/10.1016/j.ceramint.2015.01.110

### 2.4. Isolation and culture of bone marrow-derived ahMSCs

Undifferentiated multipotent *ah*MSCs were isolated from the bone marrow obtained by percutaneous direct aspiration from an iliac crest of three male human volunteers (50 ml/patient) in good physical condition. All the procedures were approved by the Institutional Ethical and Clinical Trials Committee (the Virgen de la Arrixaca University Hospital). Informed consent was obtained from all the volunteers. For the isolation of *ah*MSCs, a mononuclear cell fraction was obtained by ficoll density gradient-based separation and the cell washing closed automated SEPAX™ System (Biosafe, Eysines, Switzerland).

After seeding the mononuclear cells at a density of $1.6 \times 10^5$ cells/cm$^2$ in basal culture growth medium (GM), they were cultured at 37 °C, 5% $CO_2$ and 95% of relative humidity atmosphere to be attached undisturbed for 7 days. The GM used was α-Minimum Essential Medium (α-MEM) (Sigma-Aldrich, St Louis, MO, USA) supplemented with 10% foetal bovine serum (FBS) (Sigma-Aldrich) and penicillin G/streptomycin sulphate (100 U/ml and 100 μg/ml, respectively; Sigma-Aldrich).

### 2.5. Subcultures of ahMSCs

After 7 days, GM was renewed by removing the non-adherent hematopoietic cells and selecting the *ah*MSCs given their proven capacity of attaching to the plastic of culture flasks [11]. When the cell culture reached 85–90% confluency, cells were detached using 0.25% w/v trypsin-EDTA for 5 min, washed and seeded at $5 \times 10^3$ cells/cm$^2$.

### 2.6. ahMSCs characterisation

In order to confirm the phenotype of the cells isolated from the primary culture, and to determine possible phenotypic changes in the expression of surface markers, the adherent isolated cells, considered to be *ah*MSCs, were tested for the positive expression of markers CD73, CD90 and CD105, and also for the absence of an expression of hematopoietic markers, e.g., CD34 and CD45, using specific mouse monoclonal antibodies (all acquired from BD Biosciences (San Diego, CA, USA) Non-specific fluorescence was measured using specific isotype monoclonal antibodies. Samples were acquired in a Beckman Coulter Navios flow cytometer (Fullerton, CA, USA) and analysed with the FCS Express V3 software. Afterwards, cells were identified as *ah*MSCs.

### 2.7. Phase contrast optical microscopic observations

To control the evolution of *ah*MSCs, cultures were observed under an inverted phase-contrast light microscope (Nikkon Elipse TS, Tokyo, Japan), their morphological changes and adhesion properties on plastic (control) and their growing under the indirect effect of the tested materials were recorded. For this purpose, cells were seeded at a density of $1.0 \times 10^4$ cells/well in 24-well culture plates and were cultured in GM under the same controlled culture conditions. Then sterile biomaterial samples were incorporated into the upper chambers of an 8 μm-pore size cell culture insert (BD Bioscience) and incubated in wells in the presence of *ah*MSCs for 48 h, and for 7, 15 and 21 days.

### 2.8. Scanning electron microscopy (SEM) study of ahMSCs seeded on ceramics

To assess the continuing effect of biomaterials on the behaviour of *ah*MSCs in cell adherence and growth terms from an ultrastructural point of view, study periods of 24 h, and of 15 and 28 days were established.

The samples seeded with *ahMSCs* were removed from culture wells, rinsed with PBS and fixed with 3% glutaraldehyde in 0.1 M cacodylate buffer for 1.5 h at 4 °C. Then they were rinsed again and post-fixed in osmium tetroxide for 1 h before being dehydrated in a series of graded ethanol solutions (30, 50, 70, 90 vol%). Final drying was performed by the critical-point method (CPDO2 Balzers Union). Gold-coated specimens were examined by SEM, while samples were palladium-coated for the EDS analysis.

### 2.9. Proliferation assay

The increment in the number of cells covering the materials was evaluated spectrophotometrically by a tetrazolium salts assay (XTT), as described by Scudiero et al. [16]. Briefly, cells were seeded onto ceramics at a density of $1.0 \times 10^4$ cells/well in 96-well plates and incubated under standard conditions. XTT with phenazine methosulphate (PMS) was added to each well. After 4 h of incubation, the absorbance of the culture medium of the cells growing on ceramic pellets was measured at 450 nm in a Multiskan MCC 340 plate reader (Labsystem, CO, USA). Another series of *ah*MSCs was seeded onto plastic to be used as a quality control of the cells seeded onto bioceramics. Adherence and growth of cells were analysed at 24 h, and at 7, 15 and 28 days.

### 2.10. Cell differentiation and functionality assays/tests

It is well-known that osteocalcin (OC) production, alkaline phosphatase activity (ALP) and collagen-type I production (Col I) are osteoblast-phenotype markers. For this reason we analysed the expression of these proteins to evaluate if any differentiating effect of *ah*MSCs on osteoblasts had taken place due to the action of ceramics. The expression of characteristic components of the extracellular matrix (ECM), such as heparan-sulphate (HS) and osteopontin (OP), was also analysed, as was the presence of mineralisation nodules. Assays were conducted on days 15 and 28 of culture and were performed at least in triplicate.

#### 2.10.1. Alkaline phosphatase activity

The ALP enzyme activity of cells was determined by histochemical staining with a commercially available qualitative assay kit (the alkaline phosphatase detection kit, Millipore,

Please cite this article as: P. Mazón, et al., Human mesenchymal stem cell viability, proliferation and differentiation potential in response to ceramic chemistry and surface roughness, Ceramics International (2015), http://dx.doi.org/10.1016/j.ceramint.2015.01.110

Billerica, MA, USA). Briefly, cells were seeded at a density of $1.0 \times 10^4$ cells/well, which came into contact with the different ceramics. Afterwards, *ah*MSCs were fixed with 4% paraformaldehyde and washed in PBS. Next staining solution (Fast Red Violet with Naphthol AS-BI phosphate solution and water in a 2:1:1 ratio) was added to each coverslip and incubated in the dark at room temperature (RT) for 15 min and washed. The cells expressing ALP activity acquired a red colour.

### 2.10.2. Osteocalcin production

OC production was measured in the supernatants of *ah*MSCs cultured at a density of $1.0 \times 10^4$ cells/well, which came into contact with ceramics by removing serum from the culture medium 5 days before determinations were made. Presence of OC was determined using the Gla-type osteocalcin EIA kit (Reactiva S.A. Barcelona, Spain) following the manufacturer´s protocol. Three determinations of each sample and standard kits were made.

### 2.10.3. Calcium deposition (mineralisation)

Presence of calcium deposition or nodules of mineralisation in cultures was evaluated qualitatively by the selective binding of Alizarin Red S (Osteogenesis kit assay, Millipore) to calcium salts. Briefly, cells were seeded at a density of $1.0 \times 10^4$ cells/well. After culturing the cells that came into indirect contact with ceramics, they were washed with PBS, fixed with 8% paraformaldehyde and stained with Alizarin Red Stain Solution. Stained areas were visualised using an optical microscope.

### 2.10.4. Osteocalcine, extracellular matrix and collagen type I expression

Osteoblast-specific markers and the extracellular matrix expression were tested by immunofluorescence techniques. To carry out these assays, cells were seeded at a density of $1.0 \times 10^4$ cells/well and cultured in GM under the same controlled culture conditions. Briefly, cells were washed 3 times with PBS, and were then fixed and permeabilised with cooled Methanol–Acetone solution (1:1) at 20 °C for 10 min. Afterwards samples were blocked with blocking solution (0.1% TRITON-X, 0.3% BSA, 10% FBS in PBS 1X) for 30 min at 37 °C. Labelling was performed by incubating primary antibodies in blocking solution at 4 °C o/n, followed by incubation with a secondary antibody in blocking solution for 1 h at RT. All the primary and secondary antibodies are summarised in Table 1. The assays were conducted on day 28 of cultures and performed at least in duplicate.

Table 1
Combination of the primary and secondary antibodies (Abs) employed for the indirect immunofluorescence experiments.

| **Primary Abs** | **Dilution** |
|---|---|
| Anti-collagen type I | 1:100 |
| Anti-osteocalcin | 1:100 |
| Anti-osteopontin | 1:100 |
| Anti-heparan sulphate | 1:100 |
| **Secondary Abs** | **Dilution** |
| Alexa Fluor® 488 *goat anti-rabbit IgG* | 1:500 |
| Alexa Fluor® 488 *goat anti-rabbit IgG* | 1:500 |
| Alexa Fluor® 488 *goat anti-rabbit IgG* | 1:500 |
| Alexa Fluor® 488 *goat anti-rat IgG* | 1:500 |
| Alexa Fluor® 488 *goat anti-mouse IgG* | 1:500 |

### 2.11. Apoptosis assay (Annexin V/7-AAD staining)

In order to rule out any possible cytotoxic effects (apoptosis and necrosis) of the different biomaterials on *ah*MSCs, cells were seeded at a density of $2.0 \times 10^5$ cells/cm$^2$ in 24-well plates and cultured in GM medium for 24 h at 37 °C to allow adherence of cells. Afterwards sterile biomaterial samples were incorporated into the upper chambers of an 8 μm-pore size cell culture insert (BD Bioscience) and were incubated in wells in the presence of *ah*MSCs for 0, 12, 24 h, and for 3 and 7 days. Later cells were detached using 0.25% w/v tripsin-EDTA solution (Sigma Aldrich, Saint Louis, MO, USA), washed with PBS and stained with the Annexin-V apoptosis detection kit (BD Bioscience). The percentage of live (Annexin-V$^-$/7-AAD$^-$), early apoptotic (Annexin$^+$/7-AAD$^-$) or late apoptotic and necrotic cells (Annexin-V$^+$/7-AAD$^+$) was analysed in a Beckman Coulter Navios flow cytometer. Subsequently, percentages of each population were calculated. All the determinations were made in triplicate.

### 2.12. Si, Ca and P analyses in culture media

The cell culture media from the apoptosis assay were collected and stored at −80 °C until the analysis was performed. Changes in ionic concentration (silicon (Si), calcium (Ca) and phosphorous (P)) were measured using an Inductively Plasma Optical Emission Spectroscopy (ICP-OES, PerkinElmer Optima 2000 Waltham, MA, USA).

### 2.13. Statistical analysis

Data were analysed by one-way analysis of variance (ANOVA) followed by Tukey–Kramer multiple comparisons. In both analyses, the minimum acceptable level of significance was $p < 0.05$.

## 3. Results

### 3.1. Material characterisation

The XRD patterns of both obtained synthetic TCP and $C_2S$ showed α-TCP and γ-$C_2S$ as the only phase present, respectively. Both compounds were ground to an average particle size of 20 μm. The results of the chemical analysis by XRF for both materials are shown in Table 2. The XRD patterns of the TCP ceramics doped with 1.5 wt% $C_2S$ or 3.0 wt% $C_2S$ showed peaks

Please cite this article as: P. Mazón, et al., Human mesenchymal stem cell viability, proliferation and differentiation potential in response to ceramic chemistry and surface roughness, Ceramics International (2015), http://dx.doi.org/10.1016/j.ceramint.2015.01.110

corresponding only with αTCP (JCPDS card no. 9-348) (Fig. 1). The intensity of the peaks depended on the $C_2S$ content in αTCP. The JCPDS X-ray powder diffraction data of pure calcium phosphate and silica-doped calcium phosphate suggested that only a significant amount of a crystalline phase could give rise to the diffraction pattern. A progressive shift in the main peaks occurred in the XRD spectra obtained herein for the $C_2S$–αTCP compounds as Si content increased. For αTCP, the position of the peak was recorded at 30.8 (2$\theta$) degrees, while the peak position occurred at 31.0 (2$\theta$) degrees and 31.2 (2$\theta$) degrees for the 1.5 wt % $C_2S$–αTCP composition and the 3.0 wt% $C_2S$–αTCP composition, respectively, according to the JCPDS card 00-058-0897 for the Si-TCP compound. The peaks at about 35 (2$\theta$) degrees also appeared separated for the 1.5 wt% $C_2S$–αTCP and 3.0 wt%–$C_2S$ compositions because of the presence of silicon in their structure. The intensities of the other peaks at 12.09 (2$\theta$) and 24.10 (2$\theta$) degrees (solely characteristic of the αTCP composition) increased significantly with a rise in the $C_2S$ content in the αTCP solid solution. These results confirmed that ceramics 1.5 wt% $C_2S$–αTCP and 3.0 wt% $C_2S$–αTCP were composed of a single phase of the solid solution of $C_2S$ in αTCP, named αTCPss in this study. This finding agreed with the data reported in the literature for silicon-doped ceramics prepared by different chemical methods [17–21]. The EDX elemental analysis of the TCPss compounds showed that as Si content increased from 0.24 wt% in the 1.5 wt% $C_2S$–αTCP composition to 0.29 wt% in the 3.0 wt % $C_2S$–αTCP composition, and that a significant reduction in grain size took place from 197 nm to 129 nm, respectively.

Table 2
The X-ray fluorescence chemical analysis results of the TCP and $C_2S$ synthetic powders.

| Chemical analysis (wt%) | $Ca_3(PO_4)_2$ | $Ca_2SiO_4$ |
|---|---|---|
| CaO | 54.22 | 44.62 |
| $SiO_2$ | ND. | 55.28 |
| $P_2O_5$ | 45.74 | ND. |
| MgO | 0.33 | ND. |
| $Na_2O$ | 0.10 | ND. |
| $K_2O$ | 0.008 | ND. |
| $Fe_2O_3$ | 0.037 | ND. |
| $TiO_2$ | 0.012 | ND. |
| SrO | 0.004 | ND. |

*ND.—nondetected (below the limit of determination of the analytical method).*

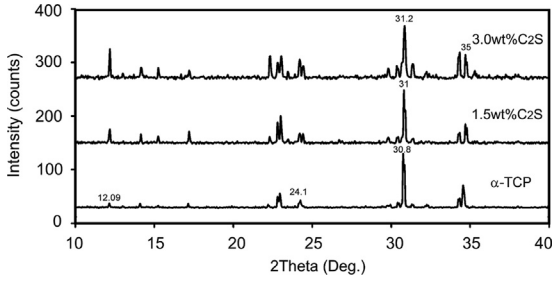


Fig. 1. X-ray diffraction patterns of the manufactured ceramic compositions.

The arithmetic mean values of each set of five measures were obtained for roughness indices $R_a$, $R_z$, and $R_q$; Ra is the arithmetic mean of the absolute values of the profile deviations (Yi) from the mean line; $R_z$ is the sum of the mean height of the five highest profile peaks and the mean depth of the five deepest profile valleys measured from a line running parallel to the mean line; $R_q$ is the square root of the arithmetic mean of the squares of profile deviations (Yi) from the mean line. The indices of roughness for the pure αTCP and αTCPss ceramics are shown in Table 3.

Fig. 2 shows a SEM micrograph of the 1.5 wt% $C_2S$–αTCP ceramic as being representative of all the compositions. The bioceramic surface of the manufactured specimens showed a rough topography (Fig. 2A). The open surface pores progressing into the material were very characteristic, with the grain structure clearly visible within larger pores. Fig. 2B depicts the polished and etched surface. No significant microstructural features are observed, except for the presence of ~20-μm closed pores. The total porosity of the samples did not change with $C_2S$ content. The image confirmed that the sample presented only one phase, with $C_2S$ in the solid solution as detected by EDX. This finding correlated well with the XRD results where only one α-TCPss phase was detected. The EDX elemental analysis of the TCPss compounds showed that Si content increased from 0.24 wt% in the 1.5 wt% $C_2S$–αTCP composition to 0.29 wt% in the 3.0 wt% $C_2S$–αTCP composition, whereas grain size reduced significantly from 197 nm to 129 nm, respectively (Table 4). Other important microstructural parameters, such as porosity, density and shrinkage, were also measured (Table 3). These parameters were also dependent on the Si content in the αTCP solid solution. When Si

Table 3
Roughness of the polished and unpolished ceramics with diamond paste.

| | αTCP | | 1.5 wt% $C_2S$–αTCP | | 3.0 wt% $C_2S$–αTCP | |
|---|---|---|---|---|---|---|
| | Polished | Unpolished | Polished | Unpolished | Polished | Unpolished |
| $R_a$ (μm) | 0.46 ± 0.04 | 2.29 ± 0.08 | 0.99 ± 0.05 | 2.02 ± 0.05 | 0.86 ± 0.04 | 2.06 ± 0.06 |
| $R_q$ (μm) | 0.67 ± 0.03 | 2.78 ± 0.08 | 1.27 ± 0.04 | 2.46 ± 0.08 | 1.03 ± 0.05 | 2.57 ± 0.08 |
| $R_z$ (μm) | 8.24 ± 0.33 | 12.52 ± 0.22 | 6.15 ± 0.23 | 10.92 ± 0.26 | 4.68 ± 0.29 | 11.69 ± 0.64 |

*Ra is the arithmetic mean of the absolute values of the profile deviations (Yi) from the mean line. Rq is the square root of the arithmetic mean of the squares of profile deviations (Yi) from the mean line. Rz is the sum of the mean height of the five highest profile peaks and the mean depth of five deepest profile valleys measured from a line parallel to the mean line.*

Please cite this article as: P. Mazón, et al., Human mesenchymal stem cell viability, proliferation and differentiation potential in response to ceramic chemistry and surface roughness, Ceramics International (2015), http://dx.doi.org/10.1016/j.ceramint.2015.01.110

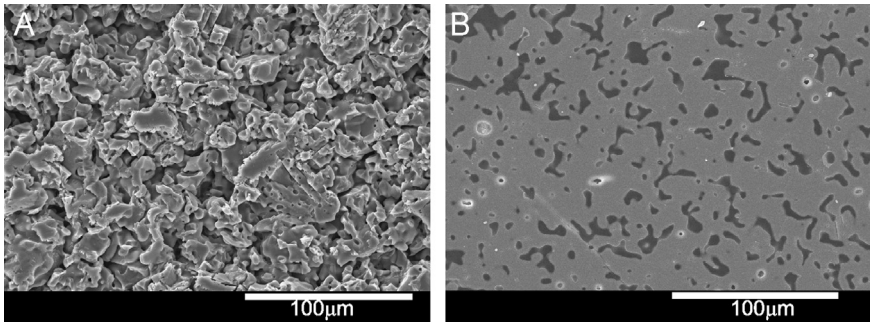


Fig. 2. SEM micrographs of the unpolished (A); polished and chemically etching (B) 1.5 wt% $C_2S$–αTCP ceramic surfaces as representative of all the ceramics.

content increased, shrinkage and density increased slightly, while porosity decreased significantly from 28% for the Si-free αTCP ceramic to 24% or 16% for the 1.5 wt% $C_2S$–αTCP ceramic or the 3.0 wt% $C_2S$–αTCP ceramic, respectively.

### 3.2. Contrast phase optical microscopy observations

After 48 h of culture, adherent *ah*MSCs were observed as individual cells or as forming aggregates or colonies, and adopted a round or slightly elongated shape (Fig. 3). At this point, no morphological differences were found between the different surfaces or ceramic compositions (control, α-TCP, 1.5 wt% $C_2S$–αTCP and 3.0 wt% $C_2S$–αTCP) (only shown for 1.5 wt% $C_2S$–αTCP). After 7 days of culture, cells grew rapidly in number, became more confluent, and adopted an elongated and polygonal shape independently of material composition or surface roughness. After 15 days, the attached *ah*MSCs showed a fibroblastic morphology, with a spindle shape that came into contact with material α-TCP and 3.0 wt% $C_2S$–αTCP, and a polygonal or cuboidal shape in material 1.5 wt% $C_2S$–αTCP, as a result of increased growth kinetics. No morphological differences were found at this time point in relation to surface roughness. After 21 days of culture, and in the presence of both smooth and rough surface-α–TCP, or 1.5 wt% $C_2S$–αTCP materials, *ah*MSCs reached 100% confluence. In contrast, and at the same time point, the cells growing on polished or unpolished-3.0 wt% $C_2S$–αTCP biomaterial did not reach the same degree of confluence compared with the other compositions (data not shown). In general, the morphological appearance of *ah*MSCs did not vary significantly as a result of the indirect action of material composition, roughness or culture time compared with the control *ah*MSCs growing in plastic. Very few small scattered deposits of refractive material were detected in cultures, mainly when using polished 1.5 wt% $C_2S$–αTCP (21 days).

### 3.3. Morphological features of cells on ceramic materials

No apparent differences in cell morphology were found on any of the materials' composition and surfaces. After the first 48 h of culture, ceramics exhibited a granular layer that covered part of the surface with spicules and small nodules (Fig. 4A and D) which, according to the SEM-EDX microanalysis, corresponded to Ca-P deposits.

Table 4
Physical characteristic of the ceramics.

| | αTCP | 1.5 wt% $C_2S$–αTCP | 3.0 wt% $C_2S$–αTCP |
|---|---|---|---|
| Grain size (nm) | 207 | 192 | 129 |
| Si (wt%) | 0.0 | $0.24 \pm 0.01$ | $0.29 \pm 0.01$ |
| Porosity (%) | 28 | 24 | 16 |
| Density (g/cm$^3$) | 2.21 | 2.26 | 2.38 |
| Shrinkage (%) | $17.7 \pm 0.5$ | $17.9 \pm 0.5$ | $18.3 \pm 0.5$ |

*Theoretical density of αTCP = 2.86 g/cm$^3$.*

After 15 days, *ah*MSCs were able to produce an extracellular matrix, which formed a fibrillar network that covered intercellular gaps. This production became even more evident when using unpolished TCPss materials, where granular material deposits of a brighter contrast were also identified within the fibrillar network (Fig. 4B). To determine its nature, the SEM–EDX microanalysis was carried out. This analysis proved that it was a calcium phosphate-based material with some traces of magnesium, similar to apatite of bone tissue. The cells in all the studied ceramics and surfaces presented similar morphologies, and some adhered cells were observed either individually or dispersed in small groups across the surface of the material.

After the 21-day period, progressive cell growth was observed on the surface of the materials, which became more evident in the unpolished TCPss materials (Fig. 4C and F). Cells almost covered the whole surface of materials to form a monolayer and showed a larger number of interconnections. An abundant extracellular matrix that covered intercellular gaps was also observed at this time. No morphological differences were observed between α-TCP and TCPss (not shown). Although their surface also exhibited the presence of cells, there were more uncoated areas on the smooth surface, and the extracellular matrix production was also smaller than for rough materials (Fig. 4F). No signs of cytotoxicity or morphological alterations were noted throughout the study, and cells grew and spread on the three materials.

### 3.4. Cell proliferation

*Ah*MSC proliferation on the different biomaterials was measured by XTT after 1, 7, 15, 21 and 28 days of culture. Fig. 5 shows the proliferation rate of the cells growing on the

Please cite this article as: P. Mazón, et al., Human mesenchymal stem cell viability, proliferation and differentiation potential in response to ceramic chemistry and surface roughness, Ceramics International (2015), http://dx.doi.org/10.1016/j.ceramint.2015.01.110

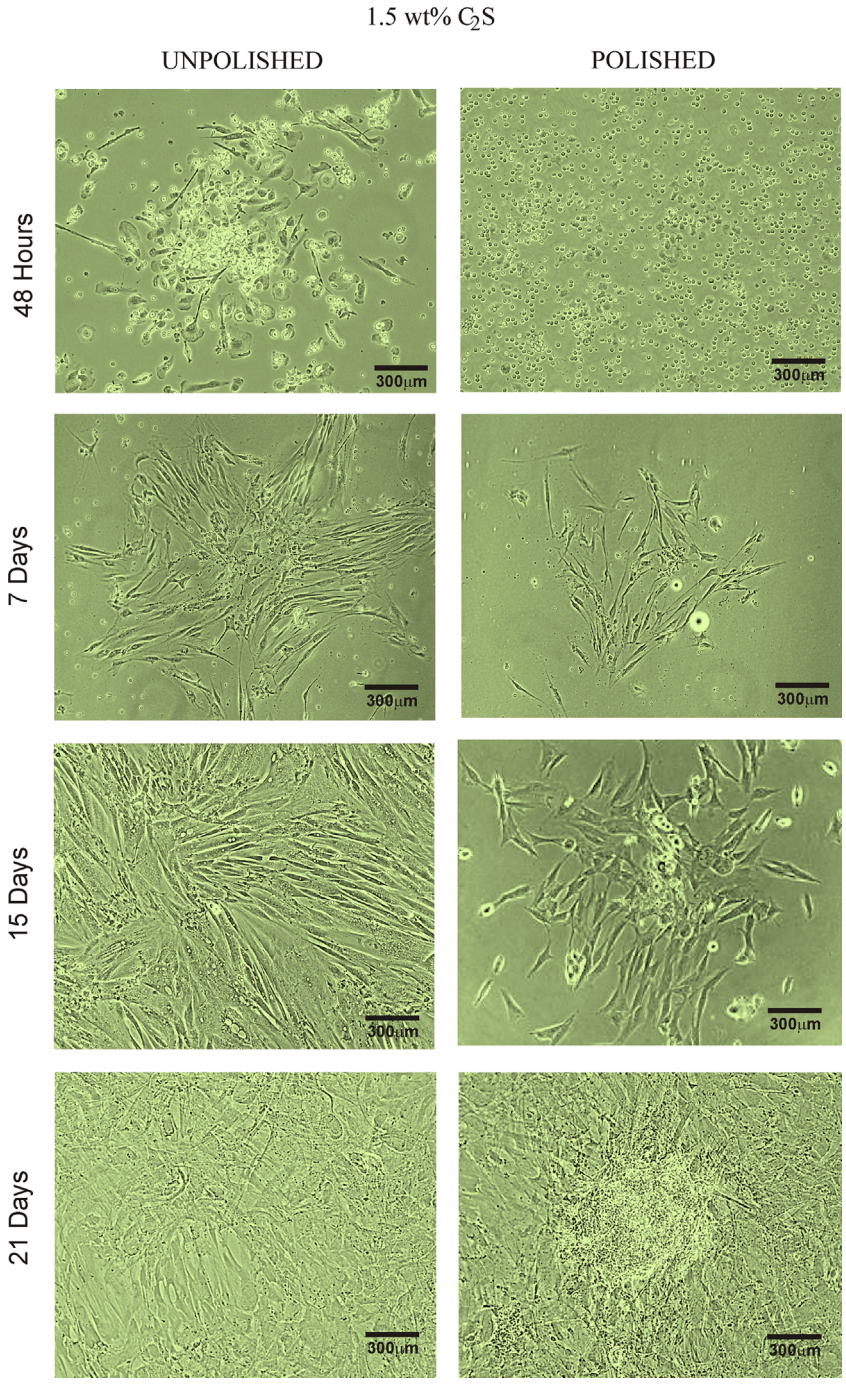


Fig. 3. Representative phase contrast microscopy images of the evolution of *ah*MSCs cultures.

unpolished and polished surfaces of the different ceramics at the indicated culture time. The XTT assays confirmed the SEM observations, where cell proliferation was predominantly higher for unpolished surfaces. Among all the biomaterials, the cell proliferation rate observed on the unpolished 1.5 wt% $C_2S$–αTCP material from 15 days of culture was significantly higher than that obtained on the polished 1.5 wt% $C_2S$–αTCP material ($p < 0.05$, $p < 0.001$). For substrate composition, the results indicate a significantly faster and higher *ah*MSCs proliferation on the 1.5 wt% $C_2S$–αTCP material (from 15 days of culture) compared to α-TCP ($^{*}p < 0.05$). At the end of the experiment (28 days of culture), the cell proliferation on the 1.5 wt% $C_2S$–αTCP material was 2-fold higher than that obtained on αTCP. Nevertheless, the proliferation shown on the 3 wt% $C_2S$–αTCP material from 21 days was significantly lower than that observed on αTCP or 1.5 wt% $C_2S$–αTCP, independently of sample roughness ($^{\Delta}p < 0.05$, $^{\Delta\Delta}p < 0.01$).

### 3.5. Cell differentiation and functionality tests

We also studied the influence of ceramic chemistry and surface roughness on the spontaneous osteogenic differentiation

Please cite this article as: P. Mazón, et al., Human mesenchymal stem cell viability, proliferation and differentiation potential in response to ceramic chemistry and surface roughness, Ceramics International (2015), http://dx.doi.org/10.1016/j.ceramint.2015.01.110

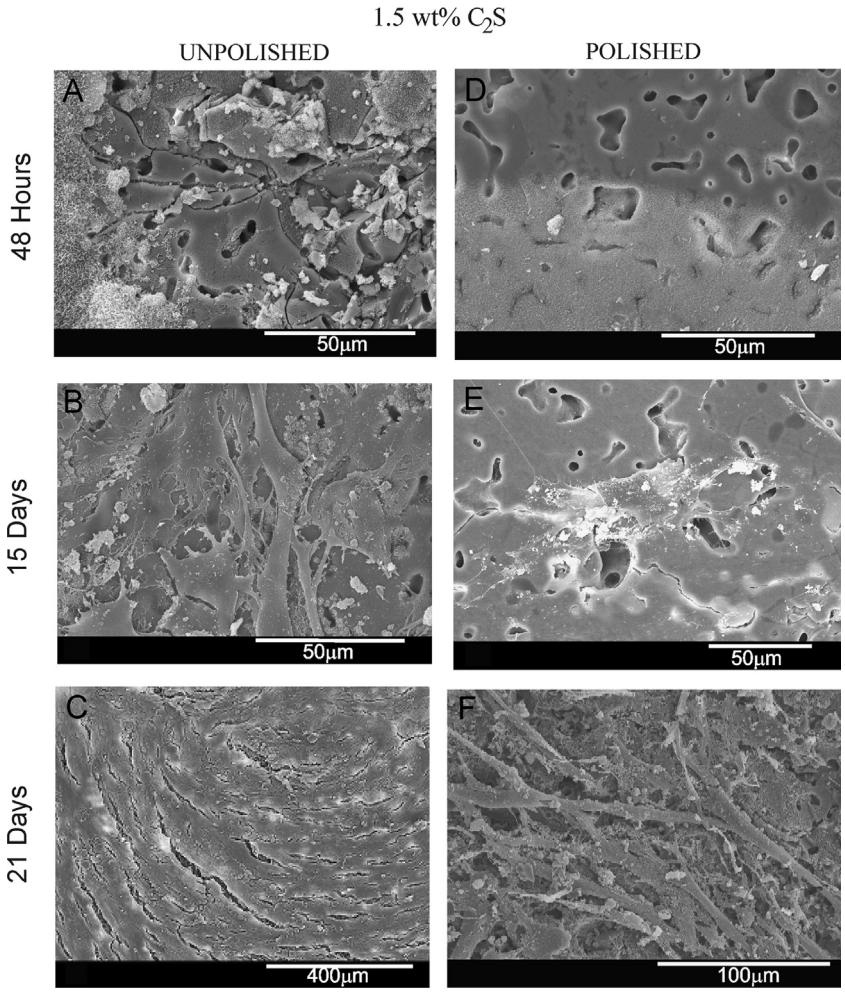


Fig. 4. SEM images of the *ah*MSCs cultured on unpolished and polished 1.5 wt% $C_2S$–αTCP ceramic surfaces in GM at 48 h, and at 15 and 21 days, as representative of all the compositions.

of *ah*MSCs by analysing alkaline phosphatase activity, and osteocalcin (OC) and collagen-type I (Col-I) expression, all the osteoblast-phenotype markers (Fig. 6A–C, respectively). We also analysed the presence of some characteristic extracellular matrix (ECM) components, such as mineral calcium deposits, which are stained bright red by the Alizarin Red Solution (Fig. 6D). The expressions of ECM proteins osteopontin (OP) and heparan sulphate (HS) were also evaluated by immunofluorescence techniques (Fig. 6E and F, respectively).

These tests are qualitative; Fig. 6 offers only the results obtained when using the unpolished 1.5 wt% $C_2S$–αTCP material because we were unable to quantify the small differences found between polished and unpolished surfaces. However, all the studied bioceramics stimulated the osteogenic differentiation of *ah*MSCs independently of their chemistry or surface roughness. After 28 days, cells were positive for alkaline phosphatase staining (Fig. 6A). The Col-I positive groups of cells augmented in both the control (plastic) and cells incubated in the presence of biomaterials, although the general aspect of the control cells was always less positive than for those cells cultivated with different biomaterials (Fig. 6C). The HS expression was very high in all the samples studied and strongly demonstrated ECM deposition because the used antibody detects the secreted form of this protein (Fig. 6F). At the same time point of our study (28 days), osteoblast-specific markers OC and OP (intracellular non-secreted proteins) were also detected in the samples incubated with different biomaterials (Fig. 6B and E, respectively). The OC and OP expressions in the control were weak or possibly non-specific expressions. Finally, the production of mineralisation nodules was clearly revealed by Alizarin Red S staining, which detected a large amount of calcium-rich deposits (Fig. 6D), properties which correlate with the findings observed by SEM and contrast phase microscopy observations. Minimal differences were noted between ceramic chemistry and surface roughness.

Fig. 7 shows the OC levels obtained when *ah*MSCs cells were seeded directly onto ceramics. The ceramic chemistry results revealed that the OC levels were significantly higher in 1.5 wt% $C_2S$ than in α-TCP pure and 3.0 wt% $C_2S$ ($^*p < 0.05$). Regarding surface roughness, when the unpolished bioceramics were used, the OC levels slightly increased, but not statistically significantly, and the OC levels obtained were higher with the 1.5 wt% $C_2S$ ceramic.

Taken together, the *ah*MSCs cultured in the presence of the α-TCP, 1.5 wt% $C_2S$ and 3.0 wt% $C_2S$ unpolished or polished

Please cite this article as: P. Mazón, et al., Human mesenchymal stem cell viability, proliferation and differentiation potential in response to ceramic chemistry and surface roughness, Ceramics International (2015), http://dx.doi.org/10.1016/j.ceramint.2015.01.110

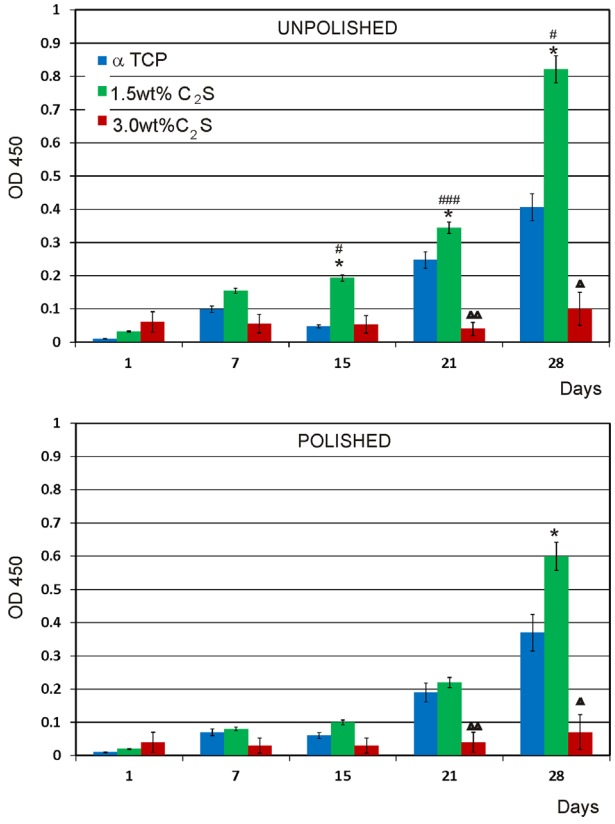


Fig. 5. Proliferation rate of *ah*MSCs, measured by tetrazolium/formazan absorbance, on the α-TCP, 1.5 wt% and 3.0 wt% $C_2S$ ceramics at different times of the study. Cell proliferation significantly increased, $^{*}p < 0.05$, or significantly decreased, $^{\Delta}p < 0.05$, $^{\Delta\Delta}p < 0.01$ compared to the proliferation obtained on α-TCP ceramics, respectively. Cell proliferation on unpolished biomaterials significantly increased, $^{\#}p < 0.05$, compared to that achieved when using polished samples.

ceramics were able to induce differentiation to osteoblasts by expressing the phenotypic characteristics of this cell type and could produce mineralised ECM.

### 3.6. Apoptosis assay

To analyse the influence of biomaterial composition and roughness on the viability of *ah*MSCs, the percentages of the live or apoptotic *ah*MSCs cultured in the presence of the indicated biomaterials for 0.5, 1, 3 and 7 days were determined (Fig. 8). For that purpose, binding of Annexin-V and 7-Amino-Actinomycin (7-AAD) was measured to determine the apoptosis stage of cells by flow cytometry. The levels of the apoptosis of *ah*MSCs did not change according to the composition or roughness of the different biomaterials assessed, except for the polished 3 wt% $C_2S$ configuration. After culturing *ah*MSCs in the presence of the unpolished (Fig. 8A) or polished (Fig. 8B) αTCP or 1.5 wt% $C_2S$ ceramics, no significant differences in the percentages of live or apoptotic cells were found for the different culture times analysed ($p > 0.05$). Conversely, the percentage of live cells cultured in the presence of the polished 3 wt% $C_2S$ biomaterial drastically lowered compared to unpolished ceramics with the same composition, especially for the longer culture time studied (7 days; $^{**}p < 0.01$).

### 3.7. Si, Ca and P analyses in culture media

The release of the soluble Si, Ca and P elements by the dissolution of ceramics in relation to roughness and chemical composition is shown in Fig. 9.

Initially the calcium (Ca) concentration significantly increased during the first 24 h of exposure to then continue to increase at a very low rate up to 7 days, independently of sample roughness. Phosphorus concentration (P) changed slightly for all the ceramics studied, which suggests that the consumption rate of P ions due to the precipitation of the Ca–P layer was similar to the P ion release rate from ceramics.

The initially higher Si content and the lower Ca levels observed in the culture medium for 3.0 wt% $C_2S$–αTCP, in comparison to 1.5 wt% $C_2S$–αTCP, indicated a faster dissolution rate of the 3.0 wt% $C_2S$–αTCP material and, therefore, a faster precipitation rate of the Ca–P on the ceramic surface. The 3.0 wt% $C_2S$–αTCP ceramic was composed of the smallest grain size in comparison to the other two materials and, therefore, presented a faster dissolution rate for elements Ca, P and Si. These differences between the dissolution rates of the various ceramics during their immersion in culture medium could potentially influence cell activity. In relation to surface roughness, all the bioceramics with considerable roughness showed a slightly higher content of Ca, P and Si ions than the smooth bioceramics in the culture medium.

## 4. Discussion

The ability to bond to bone tissue is a unique property of bioactive ceramics. Analyses of the bone-implant interface have revealed that presence of hydroxyapatite (HA) is one of the key features in the bonding zone [21–25]. Surface characteristics, which are of key relevance for designing optimal implants, have not yet been fully investigated. Bone bioactivity involves physicochemical surface reactions and cellular events, including cell attachment to adsorbed extracellular matrix proteins [26]. Substrate composition and structure are able to influence not only the kinetics of protein adsorption, but also the structure of adsorbed proteins [27].

In the present work, we examined the effect of the substrate chemistry and surface roughness of αTCP biomaterials on cellular proliferation, osteogenic differentiation and viability of cells. The cellular source used for this study was adult human mesenchymal stem cells (*ah*MSCs) stimulated *in vitro* to form osteoblastic cells. TCP ceramic supports the osteoblastic differentiation of *ah*MSCs [4,10,28]. The advantage of this methodology is that cells are of human origin and come into direct contact with biomaterial after in situ implantation. They can differentiate into various cell types depending on the surface and culture conditions [29–31].

The present work forms part of a project that studies different parameters, which may influence cell response. We thus investigated cell response on αTCP bioceramics with two

Please cite this article as: P. Mazón, et al., Human mesenchymal stem cell viability, proliferation and differentiation potential in response to ceramic chemistry and surface roughness, Ceramics International (2015), http://dx.doi.org/10.1016/j.ceramint.2015.01.110

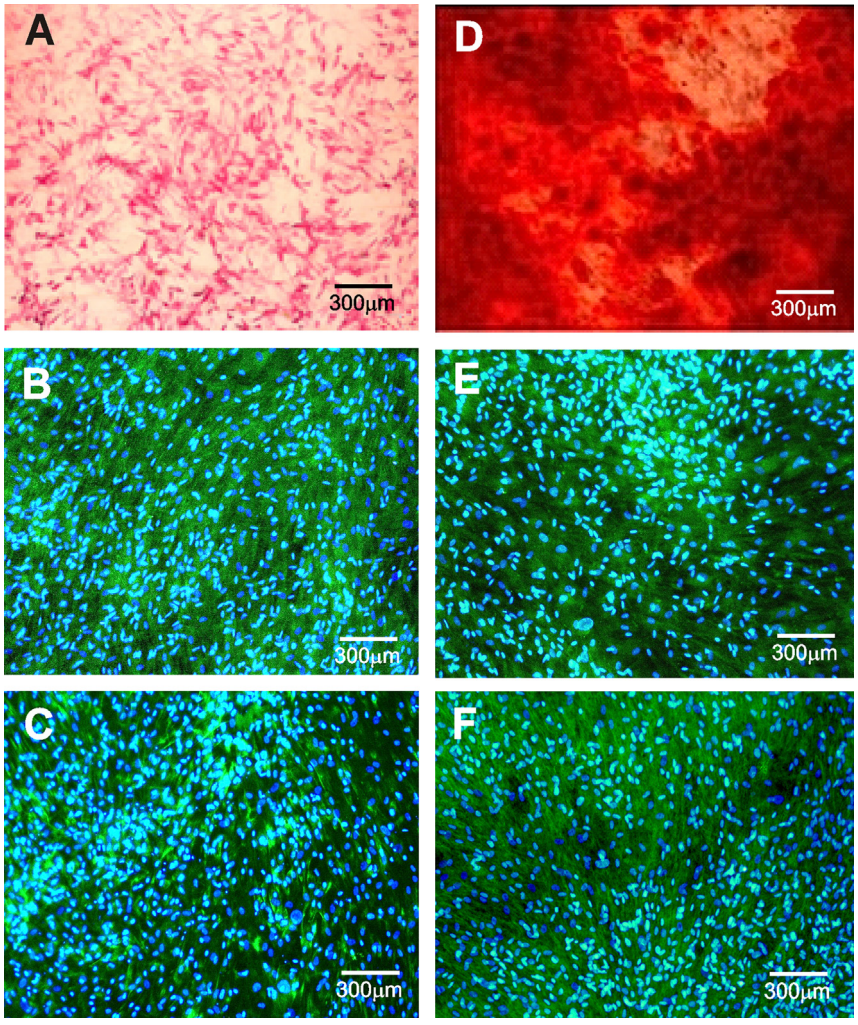


Fig. 6. Representative histochemical ALP staining, Alizarin Red staining and indirect immunofluorescence images of the *ah*MSCs cultured in the presence of unpolished 1.5 wt% $C_2S$–TCP as representative of all the compositions and surface roughnesses. (A) Alkaline phosphatase activity; (B) osteocalcin production; (C) collagen-type I production; (D) mineralisation nodules production; (E) osteopontin expression (F) heparan sulphate expression.

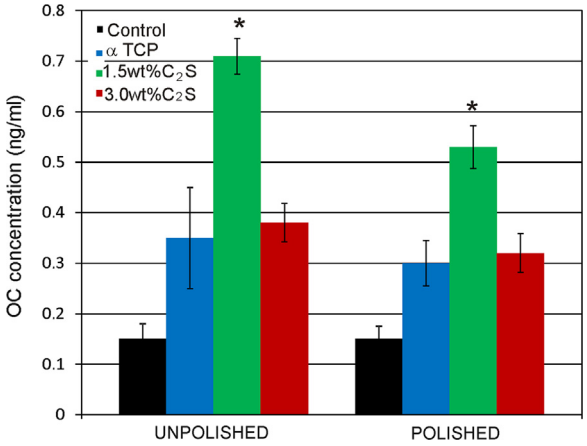


Fig. 7. Osteocalcin production by *ah*MSCs after 28 days of growth on polished and unpolished bioceramic disks. The OC concentration significantly increased, $^*p < 0.05$, according to the ANOVA.

different surface roughness values and three compositions (pure α-TCP, and αTCP doped with either 1.5 wt% or 3.0 wt% of dicalcium silicate).

It has been established that a wide range of manufactured materials with different topographies can elicit different responses on several cell types. For example, different studies into osteoblasts have reported no effect [32], a higher [33–34] or a lower level [35] of adhesion with increasing surface roughness. Our results suggest that the behaviour of ahMSCs is influenced by the surface roughness and substrate chemistry of αTCP.

The roughness obtained in our preparations consisted of a macroscopically homogenous topography with open pores. We found that when cells were elongated, they were orientated along the grooves on rough bioceramics. Yet we observed no preferential orientation of the cell in an early culture stage when the material was polished (data not shown). The roughness values for αTCP and αTCPss ceramic ranged from $0.46 \pm 0.04$ and $2.29 \pm 0.08$ μm, respectively. In the literature, Ong et al. [36] reported a roughness value of 0.67 μm, but the different treatments that these authors used produced the same roughness. Ohgushi et al. [37] reported roughness values of 0.22 μm and 0.78 μm on apatite-wollastonite glass ceramic, and they did not observe significant differences in either ALP or DNA contents. Keller et al. [38], who noticed a significantly higher level of cell

Please cite this article as: P. Mazón, et al., Human mesenchymal stem cell viability, proliferation and differentiation potential in response to ceramic chemistry and surface roughness, Ceramics International (2015), http://dx.doi.org/10.1016/j.ceramint.2015.01.110

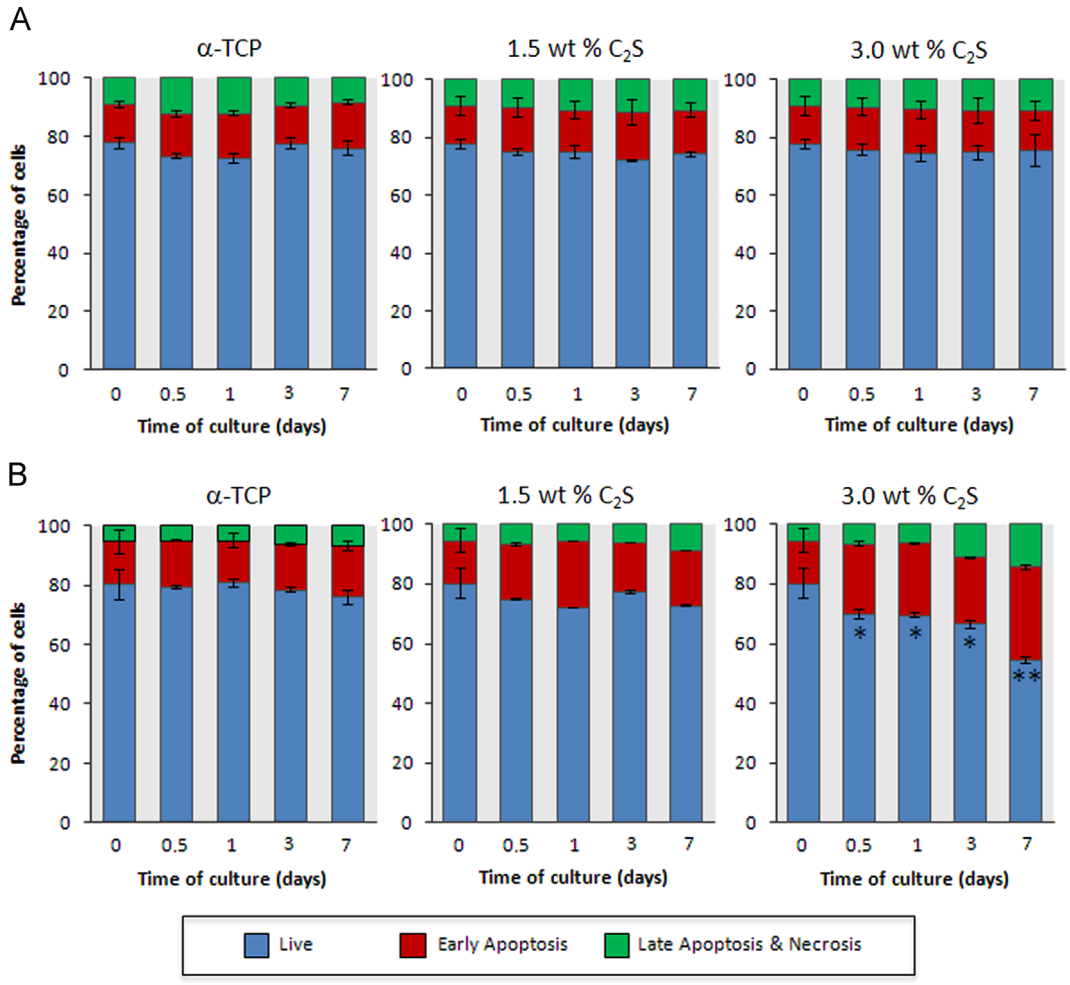


Fig. 8. Effect of bioceramics with a unpolished or a polished surface on the viability of *ah*MSCs. Mesenchimal stem cells were cultivated at 37 °C in GM medium in the absence (time of culture 0) or presence of unpolished (A) or polished bioceramics (B) with the indicated composition for 0.5, 1, 3 and 7 days. The percentage of live (Annexin-V$^-$/7-AAD$^-$), early apoptotic (Annexin +/7-AAD$^-$) or late apoptotic and necrotic cells (Annexin-V$^+$/7-AAD$^+$) was measured by flow cytometry. The mean values ± SD of the three independent experiments are shown,. $^*p < 0.05$, $^{**}p < 0.01$, $^{***}p < 0.001$, according to the ANOVA.

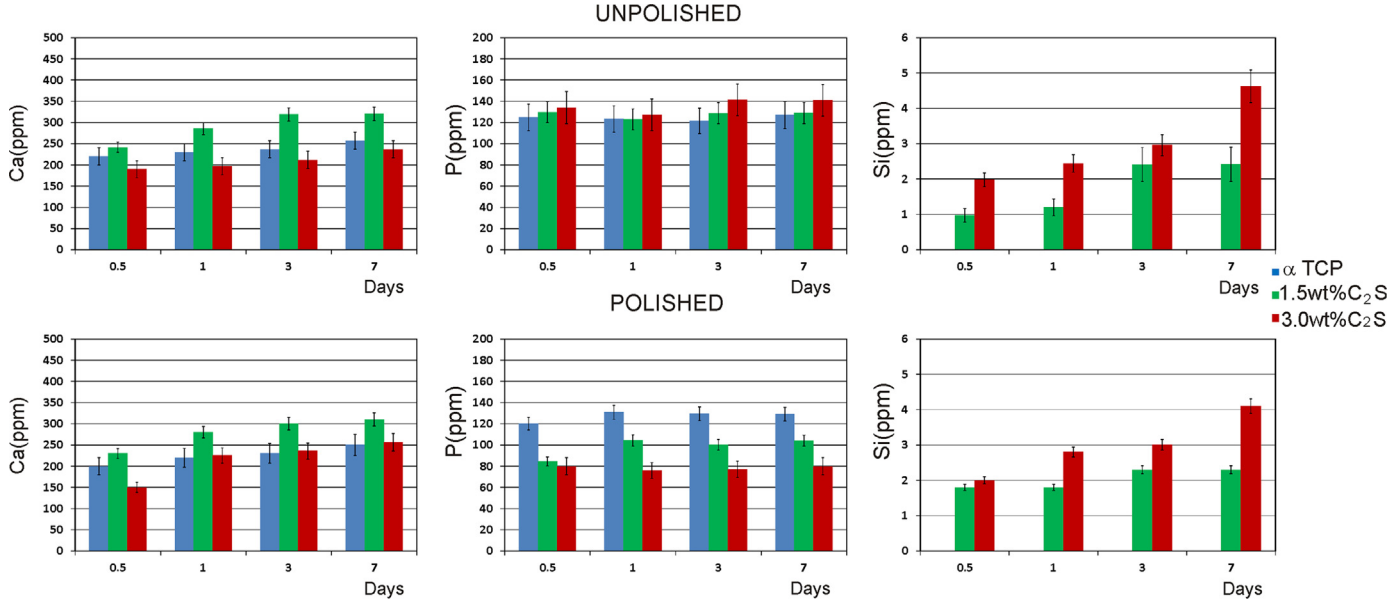


Fig. 9. Concentrations of $Si^{4+}$, $Ca^{2+}$, $HPO_4^{=}$ in the *ah*MSC culture medium after different immersion times.

Please cite this article as: P. Mazón, et al., Human mesenchymal stem cell viability, proliferation and differentiation potential in response to ceramic chemistry and surface roughness, Ceramics International (2015), http://dx.doi.org/10.1016/j.ceramint.2015.01.110

attachment on rough surfaces, did not provide surface roughness values. They also used different treatments to produce surface roughness, which could have resulted in a non-uniform surface morphology.

It has been reported that the critical event for bone bonding is cell (mesenchymal stem cells) adhesion onto the HA or TCP surface followed by osteoblastic differentiation [10,16,28,31,36]. αTCP and αTCPss surfaces displayed normal morphological features and cells were able to significantly attach and spread all the tested surfaces (Fig. 4). It is noteworthy that the growth and cellular proliferation obtained with polished αTCP and αTCPss ceramics were lesser than with roughness ceramics. Similar adhesion and proliferation results have been reported previously by other researchers [39–41]. Both mesenchymal stem cell adhesion and proliferation are sensitive surface roughness functions. In relation with the chemistry of the ceramic, the 1.5 wt% $C_2S$–αTCP material allowed better growth and cellular proliferation than the 3.0 wt% $C_2S$–αTCP or pure αTCP ceramics. When longer culture times were used, the distribution of cells over specimens was homogeneous and they were well attached as sample surfaces were uniformly colonised. This indicates that the materials developed in this study are biocompatible, and allow a high colonisation and proliferation rate.

Cell adhesion on αTCP and αTCPss surfaces can be explained by the selective adsorption of the proteins present in serum since adsorbed proteins modulate cellular interactions. El-Ghannam et al. [42] found that adsorption of serum fibronectin to the calcium phosphate surface may be responsible for enhanced osteoblast adhesion. Apart from an initial attachment enhancement, fibronectin has been found to be a survival factor for differentiated osteoblasts [43]. A direct relationship between TGF-β1 production by fibroblastic cell line MG-63 and the surface roughness of titanium (Ti) has also been found, which suggests that substrate surface roughness can modulate the activity of cells [44]. It is known that the physicochemical features of the ceramic surface can affect the reorganisation of proteins on ceramic specimens and can change the profile of adsorbed proteins [45]. Substrate type determines which integrins and extracellular matrix proteins are expressed by osteoblasts, which provides information as to how implant materials can affect osteoblast differentiation. Differences in protein adsorption can result in very distinct initial cell behaviour [46]. Thus a better understanding of the interaction among αTCP, TCPss and serum proteins is necessary.

The ability of cells to produce a mineralised extracellular matrix is important for suitable materials to be developed for bone regeneration. It is believed that Si ions play an important role in mineralisation and nodule formation. Certain concentrations of the dissolution product of silica-based biomaterials have a highly beneficial effect on cell function, which has also been demonstrated by several authors [4,10,17–20,28,32]. However, higher concentrations can cause cell death. Several markers, such as ALP activity, expression of Col-I and osteocalcin production have been used to monitor the process of differentiation of undifferentiated mesenchymal stem cells to osteoblastic linage cells *in vitro*.

The present work has demonstrated that *ah*MSCs are able to undergo a differentiation process, and has shown an osteoblastic phenotype and the ability to synthesise mineralised ECM. The effect of TCPss materials on *ah*MSCs differentiation into osteoblasts is favoured by roughness and the Si content in solid solution in TCP ceramics, by the release of Si, Ca and P ions into the medium, and also by the formation of the afore-mentioned Ca-P deposits (Fig. 4).

In the present study, we also analysed whether the roughness of the surface of different αTCP and αTCPss ceramics can influence the viability of *ah*MSC*s* cultured *in vitro*. To this end, the method of double-staining cells with Annexin-V and 7-AAD was applied. Annexin-V staining precedes loss of membrane integrity, which accompanies the latest cell death stages resulting from either apoptotic or necrotic processes. Therefore, staining with Annexin-V is used typically in combination with a vital dye, such as 7-AAD, to identify apoptosis in its different stages. We found that surface-induced apoptosis was time-, roughness- and chemistry-dependent since the percentage of apoptotic *ah*MSCs cultured in the presence of polished 3.0 wt% $C_2S$–αTCP ceramics progressively and significantly increased from 12 h to 7 days. The cytocompatibility of the remaining biomaterials was then confirmed by these results as they preserved cellular viability.

The literature contains many data which indicate that Si concentrations $<19$ ppm or Ca concentrations $\sim$200–500 ppm can favour osteoblastic differentiation [47–51] and cell viability. Thus it seems that there is an optimal concentration range for these soluble factors to stimulate cell differentiation.

When the unpolished 1.5 wt% $C_2S$–αTCP ceramic was used, the Si concentration increased from $\sim$0.97 to 2.42 ppm in 7 days (Fig. 9), while the Ca concentration increased from $\sim$241.4 to 320 ppm. The initial Si and Ca concentrations produced by 3 wt% $C_2S$–αTCP differed vastly, with a much higher initial Si concentration ($\sim$1.98 ppm) and a lower Ca concentration (190 ppm). Subsequently, the Ca concentration remained lower in 3.0 wt% $C_2S$–αTCP, although the P concentration increased compared to 1.5 wt% $C_2S$–αTCP (140.87 ppm and 129.06 ppm, respectively). These changes in the soluble factor concentrations may affect cell proliferation, and also OC production, which was lower during 3.0 wt% $C_2S$–αTCP exposure than for 1.5 wt% $C_2S$–αTCP. The behaviour of the polished ceramics was similar to that of the ceramics with an unpolished or rough surface, but the ion concentration was lower. This means that the dissolution rate of materials was slower in the polished than in the unpolished or rough surfaces and, therefore, the precipitation rate of Ca-P on the ceramic surface was slower. Our results also indicate that the optimal concentration ranges of soluble elements might be needed in the media to ensure cell growth proliferation and osteogenic differentiation. The optimal concentration range concept has been supported by a previous in vivo study using New Zealand rabbits [5,8,51], which showed that 1.5 wt% $C_2S$–TCP ceramics significantly supported more bone in-growth than 3 wt% $C_2S$–TCP ceramics. The cell growth and proliferation assays allow us to conclude that different soluble factors can have distinct influences and can act cooperatively or in opposition.

## 5. Conclusions

This study has investigated the effect of substrate chemistry and surface roughness on *ah*MSCs' proliferation, functionality,

Please cite this article as: P. Mazón, et al., Human mesenchymal stem cell viability, proliferation and differentiation potential in response to ceramic chemistry and surface roughness, Ceramics International (2015), http://dx.doi.org/10.1016/j.ceramint.2015.01.110

induction of apoptosis, osteoblastic differentiation and mineralised bone matrix deposition given its potential use in bone tissue engineering.

In addition to substrate chemistry, we conclude that surface roughness can affect cellular behaviour by enhancing cell adhesion and proliferation. The results consistently indicate that a rough surface, together with an appropriate Si concentration in ceramics, are effective enough to support the proliferation of *ah*MSCs. The biocompatibility of α-TCP and TCPss ceramics was dependent on their surface topography and initial composition. Cell adhesion and cell proliferation were better in the 1.5 wt% $C_2S$–TCP unpolished ceramic. However, it should be noted that all the ceramics allowed cells to spread, and cells were able to come into close contact with materials by adopting a spindle, polygonal and flattened morphology, and by showing numerous filopodia that anchor cells to ceramics. The results obtained in the proliferation and viability experiments suggest that the materials developed in this study are not cytotoxic, support a strong adhesion of *ah*MSCs on their surfaces, and promote quick proliferation and extracellular matrix production.

These results extend current knowledge about surface-mediated cell functions and provide useful information for the design criteria of next-generation biomaterials for various biomedical applications, such as tissue engineering and regenerative medicine.

## Acknowledgements

Part of this work has been supported by a Spanish Ministry of Economy and Competitiveness (MINECO) contract grant number: MAT2013-48426-C2-2-R.

## References

[1] J.M. Fernandez-Pradas, P. Serra, J.M. Morenza, P.N. De Aza, Pulser laser deposition os pseudowollastonite coatings, Biomaterials 23 (2002) 2057–2061.
[2] A.E. Porter, N. Patel, J.N. Skepper, S.M. Best, W. Bonfield, Comparison of in vivo dissolution processes in hydroxyapatite and silicon-substituted hydroxyapatite bioceramics, Biomaterials 24 (2003) 4609–4620.
[3] S.M. Best, A.E. Porter, E.S. Thian, J. Huang, Bioceramics: past, present and for the future, J. Eur. Ceram. Soc. 28 (2008) 1319–1327.
[4] I.M. Martínez, P.A. Velasquez, L. Meseguer-Olmo, P.N. De Aza, Production and study of *in vitro* behaviour of monolithic α-tricalcium phosphate based ceramics in the system $Ca_3(PO_4)_2$–$Ca_2SiO_4$, Ceram. Int. 37 (2011) 2527–2535.
[5] J.E. Mate-Sanchez de Val, J.L. Calvo-Guirado, R.A. Delgado-Ruiz, Ma. P. Ramirez-Fernandez, I.M. Martinez, J.M. Granero-Marin, B. Negri, F. Chiva-Garcia, J.M. Martinez-Gonzalez, P.N. de Aza, New block graft of α-TCP with silicon in critical size defects in rabbits: chemical characterization, histological, histomorphometric and micro-CT study, Ceram. Int. 38 (2012) 1563–1570.
[6] L. Hench, Bioceramics: from concept to clinic, J. Am. Ceram. Soc. 74 (1991) 1487–1510.
[7] A.M. Minarelli-Gaspar, S. Saska, R.G. Carrodeguas, A.H. De, Az, P. Pena, P.N. De Aza, S. De Aza, Biological response to wollastonite doped α-tricalcium phosphate implants in hard and soft tissues in rats, Key Eng. Mater. 396–398 (2009) 7–10.
[8] J.E. Mate-Sanchez de Val, J.L. Calvo-Guirado, R.A. Delgado-Ruiz, Ma. P. Ramirez-Fernandez, B. Negri, M. Abboud, I.M. Martinez, P.N. de Aza, Physical properties, mechanical behavior, and electron microscopy study of a new α-TCP block graft with silicon in an animal model, J. Biomed. Mater. Res. A 100 (12) (2012) 3446–3454.
[9] P.N. De Aza, A.H. De Aza, A. Herrera, F.A. Lopez-Prats, P. Pena, The influence of sterilization technique on *in vitro* bioactivity of pseudowollastonite ceramic, J. Am. Ceram. Soc. 89 (8) (2006) 2619–2624.
[10] L. Meseguer-Olmo, S. Aznar-Cervantes, P. Mazón, P.N. De Aza, In vitro behaviour of adult mesenchymal stem cells of human origin seeded on a novel bioactive ceramics in the $Ca_3(PO_4)_2$–$Ca_2SiO_4$ system, J. Mater. Sci. Mater. Med. 23 (12) (2012) 3003–3014.
[11] J.R. Mauney, J. Blumberg, M. Pirun, V. Volloch, G. Vunjak-Novakovic, D.L. Kaplan, Osteogenic differentiation of human bone marrow stromal cells on partially demineralized bone scaffolds *in vitro*, Tissue Eng. 10 (2004) 81–92.
[12] K.T. Bowers, J.C. Keller, B.A. Randolph, D.G. Wick, C.M. Michaels, Optimization of surface micromorphology for enhanced osteoblast responses *in vitro*, Int. J. Oral Maxillofac. Implants 7 (1992) 302–310.
[13] A.S.G. Curtis, C.D.W. Wilkinson, Reactions of cells to topography, J. Biomater. Sci. Polym. Ed. 9 (1998) 1313–1329.
[14] I.M. Martínez, P.A. Velasquez, P.N. De Aza, Synthesis and stability of α-tricalcium phosphate doped with dicalcium silicate in the system $Ca_3(PO_4)_2$–$Ca_2SiO_4$, Mater. Charact. 61 (2010) 761–767.
[15] I.M. Martinez, P.A. Velasquez, P.N. De Aza, The sub-system α-$TCP_{ss}$-silicocarnotite within the binary system $Ca_3(PO_4)_2$–$Ca_2SiO_4$, J. Am. Ceram. Soc. 95 (3) (2012) 1112–1117.
[16] D.A. Scudiero, R.H. Shoemaker, K.D. Paul, A. Monks, S. Tiemey, T.H. Nofziger, M.J. Currens, D. Seniff, M.R. Boyd, Evaluation of a soluble tetrazolium/formazan assay for cell growth and drug sensitivity in culture using human and other tumour cell lines, Cancer Res. 48 (1988) 4827–4833.
[17] R.G. Carrodeguas, A.H. De Aza, J. Jiménez, P.N. De Aza, P. Pena, A. Lopez-Bravo, S. De Aza, Preparation and *in vitro* characterization of wollastonite doped tricalcium phosphate ceramics, Key Eng. Mater. 361-363 (2008) 237–240.
[18] M. Bohner, Silicon-substituted calcium phosphates—a critical view, Biomaterials 30 (2009) 6403–6406.
[19] J.W. Reid, L. Tuc, M. Sayer, K. Fargo, J.A. Hendry, Synthesis and characterization of single-phase silicon-substituted α-tricalcium phosphate, Biomaterials 27 (2006) 2916–2925.
[20] M. Sayera, A.D. Stratilatova, J. Reida, L. Calderina, M.J. Stotta, X. Yina, M. MacKenzieb, T.J.N. Smith, J.A. Hendryc, S.D. Langstaff, Structure and composition of silicon-stabilized tricalcium phosphate, Biomaterials 24 (2003) 369–382.
[21] P. Ducheyne, J. Beight, J. Cuckler, B. Evans, S. Radin, Elect of calcium-phosphate coating characteristics on early postoperative bone tissue ingrowth, Biomaterials 11 (1990) 531–540.
[22] P. Ducheyne, J.M. Cuckler, Bioactive ceramic prosthetic coatings, Clin. Orthop. Relat. Res. 276 (1992) 102–114.
[23] J.D. de Bruijn, Y.P. Bovell, van C.A. Blitterswijk, Structural arrangements at the interface between plasma sprayed calciumphosphates and bone, Biomaterials 15 (1994) )543–)550.
[24] J.D. de Bruijn, T.S. Flach, H. Leenders, J. van de Brink, C.A. van Blitterswijk, Degradation and interface characteristics of plasma sprayed hydroxyapatite coatings with diferent crystallinities, in: T. Yamamuro, T. Kokubo, T. Nakamura (Eds.), Bioceramics, vol. 5, Kobunshi Kankokai, Kyoto, 1992, pp. 291–308.
[25] S.H. Maxian, J.P. Zawadski, M.G. Dunn, In vitro evaluation of amorphous calcium-phosphate and poorly crystallized hydroxyapatite coating on titanium implants, J. Biomed. Mater. Res. 27 (1993) 111–117.
[26] A.J. Garcia, P. Ducheyne, D. Boettinger, Quantification of cell adhesion using a spinning disc device and application to surface reactive materials, Biomaterials 18 (16) (1997) 1091–1098.
[27] K.K. Zeng, W.R. Chittur, Lacefield, analysis of bovine serum albumin adsorption on calcium phosphate and titanium surfaces, Biomaterials 20 (1999) 377–384.
[28] L. Meseguer-Olmo, A. Bernabeu-Esclapez, E. Ros-Martinez, S. Sanchez-Salcedo, S. Padilla, A.I. Martin, et al., In vitro behaviour of adult mesenchymal stem cells seeded on a bioactive glass ceramic in the $SiO_2$–$CaO$–$P_2O_5$ system, Acta Biomater. 4 (2008) 1104–1113.

Please cite this article as: P. Mazón, et al., Human mesenchymal stem cell viability, proliferation and differentiation potential in response to ceramic chemistry and surface roughness, Ceramics International (2015), http://dx.doi.org/10.1016/j.ceramint.2015.01.110

[29] R.J. Deans, A.B. Moseley, Mesenchymal stem cells: biology and potential clinical uses, Exp. Hematol. 28 (8) (2000) 875–884.
[30] P. Muller, U. Bulnheim, A. Diener, F. Luthen, M. Teller, E.D. Klinkenberg, et al., Calcium phosphate surfaces promote osteogenic differentiation of mesenchymal stem cells, J. Cell. Mol. Med. 12 (2008) 281–291.
[31] L. Saldana, S. Sanchez-Salcedo, I. Izquierdo-Barba, F. Bensiamar, L. Munuera, M. Vallet-Regi, et al., Calcium phosphate-based particles influence osteogenic maturation of human mesenchymal stem cells, Acta Biomater. 5 (2009) 1294–1305.
[32] J.D. Ballard, Investigation of Cell Adhesion to Silica Nanoparticle-decorated Surfaces and the Associated Protein-mediated Mechanisms (Doctoral Thesis), Rensselaer Polytechnic Institute, Troy, NY, 2005.
[33] T.J. Webster, R.W. Siegel, R. Bizios, Osteoblast adhesion on nanophase ceramics, Biomaterials 20 (1999) 1221–1227.
[34] K. Anselme, M. Bigerelle, Topography effects of pure titanium substrates on human osteoblast long-term adhesion, Acta Biomater. 1 (2005) 211–222.
[35] N. Nishimura, T. Kawai, Effect of microstructure of titanium surface on the behaviour of osteogenic cell line MC3T3-E1, J. Mater. Sci. Mater. Med. 9 (1998) 99–102.
[36] J.L. Ong, C.A. Hoppe, H.L. Cardenas, R. Cavin, D.L. Carnes, A. Sogal, G.N. Raikar, Osteoblast precursor cell activity on HA surfaces of deferent treatments, J. Biomed. Mater. Res. 29 (3) (1998) 389–401.
[37] H. Ohgushi, Y. Dohi, T. Yoshikawa, S. Tamai, S. Tabata, K. Okunaga, T. Shibuya, Osteogenic differentiation of cultured marrow stromal stem cells on the surface of bioactive glass ceramics, J. Biomed. Mater. Res. 32 (3) (1996) 341–348.
[38] J.C. Keller, J.G. Collins, G.G. Niederauer, T.D. McGee, In vitro attachment of osteoblast-like cells to osteoceramic materials, Dent. Mater. 13 (1997) 62–68.
[39] M. Okumura, H. Ohgushi, Y. Dohi, T. Katuda, S. Tamai, H.K. Koerten, S. Tabata, Osteoblastic phenotype expression on the surface of hydroxyapatite ceramics, J. Biomed. Mater. Res. 37 (1997) 122–129.
[40] M. Hott, B. Noel, D. Bernache-Assolant, C. Rey, P.J. Marie, Proliferation and differentiation of human trabecular osteoblastic cells on hydroxyapatite, J. Biomed. Mater. Res. 34 (1997) 508–516.
[41] D.A. Puleo, L.A. Holleran, R.H. Doremus, R. Bizios, Osteoblast responses to opthopaedic implant materials *in vitro*, J. Biomed. Mater. Res. 25 (1991) 711–723.
[42] A. El-Ghannam, P. Ducheyne, I.M. Shapiro, Effect of serum proteins on osteoblast adhesion to surface-modified bioactive glass and hydroxyapatite, J. Orthop. Res. 17 (3) (1999) 340–345.
[43] R.K. Globus, S.B. Doty, J.C. Lull, E. Holmuhamedov, M.J. Humphries, C.H. Damsky, Fibronectin is a survival factor for differentiated osteoblasts, J. Cell Sci. 111 (1998) 1385–1393.
[44] K. Kieswetter, Z. Schwartz, T.W. Hummert, D.L. Cohran, J. Simpson, D.D. Dean, B.D. Boyan, Surface roughness modulates the local production of growth factors and kytokines by osteoblast-like MG-63 cells, J. Biomed. Mater. Res. 32 (1996) 55–63.
[45] A. Laczka-Osyczka, M. Lazka, S. Kasugai, K. Ohya, Behavior of bone marrow cells cultured on three different coatings of gel derived bioactive glass–ceramics at early stages of cell differentiation, J. Biomed. Mater. Res. 42 (1998) 433–442.
[46] J. Sun, L. Wei, X. Liu, Influences of ionic dissolution products of dicalcium silicate coating on osteoblastic proliferation, differentiation and gene expression, Acta Biomater. 5 (2009) 1284–1293.
[47] I.D. Xynos, A.J. Edgar, L.D.K. Buttery, L.L. Hench, J.M. Polak, Ionic products of bioactive glass dissolution increase proliferation of human osteoblasts and induce insulin-like growth factor II mRNA expression and protein synthesis, Biomed. Biophys. Res. Commun. 276 (2000) 461–465.
[48] V. Murashov, M. Harper, E. Demchuk, Impact of silanol surface density on the toxicity of silica aerosols measured by erythrocyte haemolysis, J. Occup. Environ. Hyg. 3 (2006) 718 (-3).
[49] Z. Elias, O. Poirot, M.C. Daniere, Cytotoxic and transforming effects of silica particles with different surface properties in Syrian hamster embryo (SHE) cells, Toxicol. In Vitro 14 (2000) 409–722.
[50] S. Ming-You, D. Shinn-Jyh, Ch. Hsien-Chang, The role of silicon in osteoblast-like cell proliferation and apoptosis, Acta Biomater. 7 (2011) 2604–2614.
[51] P. Velasquez, Z.B. Luklinska, L. Meseguer-Olmo, J.E. Mate-Sanchez de Val, R. A. Delgado-Ruiz, J.L. Calvo-Guirado, M.a.P. Ramirez-Fernandez, P.N. de Aza, αTCP ceramic doped with dicalcium silicate for bone regeneration applications prepared by powder metallurgy method. In vitro and in vivo studies, J. Biomed. Mater. Res. A 101 (7) (2013) 1943–1954.

Please cite this article as: P. Mazón, et al., Human mesenchymal stem cell viability, proliferation and differentiation potential in response to ceramic chemistry and surface roughness, Ceramics International (2015), http://dx.doi.org/10.1016/j.ceramint.2015.01.110